
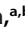


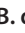






# Interplay among Different Fosfomycin Resistance Mechanisms in *Klebsiella pneumoniae*

 M. Ortiz-Padilla,<sup>a,b,c,d</sup>  I. Portillo-Calderón,<sup>a,c,d</sup>  B. de Gregorio-Iaria,<sup>a</sup>  J. Blázquez,<sup>d,e</sup>  J. Rodríguez-Baño,<sup>a,c,d,f</sup>  A. Pascual,<sup>a,b,c,d</sup>  
 J. M. Rodríguez-Martínez,<sup>b,c,d</sup>  F. Docobo-Pérez<sup>b,c,d</sup>

<sup>a</sup>Unidad de Gestión Clínica de Enfermedades Infecciosas, Microbiología y Medicina Preventiva, Hospital Universitario Virgen Macarena, Seville, Spain

<sup>b</sup>Departamento de Microbiología, Universidad de Sevilla, Seville, Spain

<sup>c</sup>Instituto de Biomedicina de Sevilla IBIS, HUVH/HUVR/CSIC/Universidad de Sevilla, Seville, Spain

<sup>d</sup>Red Española de Investigación en Patología Infecciosa (REIPI RD16/0016), Instituto de Salud Carlos III, Madrid, Spain

<sup>e</sup>Centro Nacional de Biotecnología, Madrid, Spain

<sup>f</sup>Departamento de Medicina, Universidad de Sevilla, Seville, Spain

J. M. Rodríguez-Martínez and F. Docobo-Pérez contributed equally as senior coauthors.

**ABSTRACT** The objectives of this study were to characterize the role of the *uhpT*, *glpT*, and *fosA* genes in fosfomycin resistance in *Klebsiella pneumoniae* and evaluate the use of sodium phosphonoformate (PPF) in combination with fosfomycin. Seven clinical isolates of *K. pneumoniae* and the reference strain (ATCC 700721) were used, and their genomes were sequenced.  $\Delta uhpT$ ,  $\Delta glpT$ , and  $\Delta fosA$  mutants were constructed from two isolates and *K. pneumoniae* ATCC 700721. Fosfomycin susceptibility testing was done by the gradient strip method. Synergy between fosfomycin and PPF was studied by checkerboard assay and analyzed using SynergyFinder. Spontaneous fosfomycin mutant frequencies at 64 and 512 mg/liter, *in vitro* activity using growth curves with fosfomycin gradient concentrations (0 to 256 mg/liter), and time-kill assays at 64 and 307 mg/liter were evaluated with and without PPF (0.623 mM). The MICs of fosfomycin against the clinical isolates ranged from 16 to  $\geq 1,024$  mg/liter. The addition of 0.623 mM PPF reduced fosfomycin MIC between 2- and 8-fold. Deletion of *fosA* led to a 32-fold decrease. Synergistic activities were observed with the combination of fosfomycin and PPF (most synergistic area at 0.623 mM). The lowest fosfomycin-resistant mutant frequencies were found in  $\Delta fosA$  mutants, with decreases in frequency from  $1.69 \times 10^{-1}$  to  $1.60 \times 10^{-5}$  for 64 mg/liter of fosfomycin. In the final growth monitoring and time-kill assays, fosfomycin showed a bactericidal effect only with the deletion of *fosA* and not with the addition of PPF. We conclude that *fosA* gene inactivation leads to a decrease in fosfomycin resistance in *K. pneumoniae*. The pharmacological approach using PPF did not achieve enough activity, and the effect decreased with the presence of fosfomycin-resistant mutations.

**KEYWORDS** *Klebsiella pneumoniae*, antimicrobial resistance, fosfomycin

The reported worldwide increase in antibiotic resistance, together with the shortage of new active drugs, has made it necessary to reuse old antimicrobial agents as an alternative strategy (1, 2). As a result, interest in fosfomycin has increased, with the aim of obtaining a better understanding of its pharmacokinetic (PK) and pharmacodynamic (PD) properties and its effectiveness in difficult-to-treat infections caused by multidrug-resistant *Enterobacteriaceae* (3, 4).

Extended-spectrum beta-lactamase (ESBL)-producing *Klebsiella pneumoniae* infections are particularly worrisome, as the incidence of such infections has increased dramatically, with limited therapeutic options for patients (5). Fosfomycin is an antimicrobial currently approved in several countries for treating uncomplicated urinary tract infections caused by *Enterobacteriales*, with activity against multidrug-resistant *K. pneumoniae* strains (6).

**Citation** Ortiz-Padilla M, Portillo-Calderón I, de Gregorio-Iaria B, Blázquez J, Rodríguez-Baño J, Pascual A, Rodríguez-Martínez JM, Docobo-Pérez F. 2021. Interplay among different fosfomycin resistance mechanisms in *Klebsiella pneumoniae*. *Antimicrob Agents Chemother* 65:e01911-20. <https://doi.org/10.1128/AAC.01911-20>.

**Copyright** © 2021 American Society for Microbiology. All Rights Reserved.

Address correspondence to F. Docobo-Pérez, [fdocobop@yahoo.es](mailto:fdocobop@yahoo.es).

**Received** 4 September 2020

**Returned for modification** 19 October 2020

**Accepted** 18 December 2020

**Accepted manuscript posted online** 23 December 2020

**Published** 17 February 2021

**TABLE 1** Fosfomycin MIC by gradient strip assay, with and without the addition of 0.623 mM PPF and amino acid modifications in fosfomycin resistance-related proteins relative to reference strain *K. pneumoniae* ATCC 700721<sup>a</sup>

Strain	MIC (mg/liter)		Mutation					
	Without PPF	With PPF	<i>glpT</i>	<i>uhpT</i>	<i>fosA</i>	<i>ptsI</i>	<i>uhpB</i>	<i>uhpC</i>
<b>ATCC 700721</b>	32	8						
ATCC 700721 $\Delta$ <i>fosA</i>	1	2			$\Delta$ <i>fosA</i>			
ATCC 700721 $\Delta$ <i>glpT</i>	32	8	$\Delta$ <i>glpT</i>					
ATCC 700721 $\Delta$ <i>uhpT</i>	$\geq 1,024$	$\geq 1,024$		$\Delta$ <i>uhpT</i>				
<b>Kp12</b>	32	4		<b>A462T</b>		<b>N174K</b>		<b>L337M</b>
Kp12 $\Delta$ <i>fosA</i>	1	4		A462T	$\Delta$ <i>fosA</i>	N174K		L337M
Kp12 $\Delta$ <i>glpT</i>	32	8	$\Delta$ <i>glpT</i>	A462T		N174K		L337M
Kp12 $\Delta$ <i>uhpT</i>	$\geq 1,024$	$\geq 1,024$		$\Delta$ <i>uhpT</i>		N174K		L337M
<b>Kp142</b>	32	8		<b>A462T</b>		<b>N174K</b>		<b>L337M</b>
Kp142 $\Delta$ <i>fosA</i>	1	8		A462T	$\Delta$ <i>fosA</i>	N174K		L337M
Kp142 $\Delta$ <i>glpT</i>	32	16	$\Delta$ <i>glpT</i>	A462T		N174K		L337M
Kp142 $\Delta$ <i>uhpT</i>	$\geq 1,024$	$\geq 1,024$		$\Delta$ <i>uhpT</i>		N174K		L337M
Kp28	32	4		A462T		N174K		L337M
Kp58	32	16	A261_N262insA	A462T		N174K		L337M
Kp86	$\geq 1,024$	256	I260_A261del	A462T	D138E	N174K		L337M
Kp88	16	2	A261_N262insA	A462T		N174K		L337M
Kp108	$\geq 1,024$	128	Y258_I259insA	A462T		N174K	T140A	L337M

<sup>a</sup>Data for wild-type ATCC 700721, Kp12, and Kp142 are in bold. *ins* and *del*, insertion and deletion, respectively.

Fosfomycin disrupts the first step in peptidoglycan biosynthesis by inhibiting the UDP-*N*-acetylglucosamine-3-enolpyruvyltransferase (MurA) enzyme leading to cell death. To carry out its activity, fosfomycin enters the bacteria via the membrane transporters UhpT (a hexose phosphate transporter) and GlpT (glycerol-3-phosphate transporter) (7). The loss of function of these transporters or genes involved in their regulation is the most common mechanism of resistance in *Escherichia coli* clinical isolates (8). Together with these resistance mechanisms, chromosomal or plasmid-borne fosfomycin-inactivating enzymes are present in many Gram-negative bacteria (9). The *fosA* gene encodes a metallo-glutathione *S*-transferase, widely distributed in the genomes of Gram-negative bacteria, mostly those belonging to the family *Enterobacteriales*, such as *K. pneumoniae*. Plasmid-encoded or chromosomal *fosA* transformed into high-copy-number plasmids has been shown to confer high-level fosfomycin resistance (9, 10). The enzyme activity of this protein is reduced by sodium phosphonoformate (PPF), a pyrophosphate analogue used for the treatment of cytomegalovirus and herpes simplex virus due to its capacity to inhibit viral DNA polymerases (11). It has been used to detect plasmid-borne *fosA* (11), but its antimicrobial activity in combination with fosfomycin against *fosA*-bearing strains has also been explored (12).

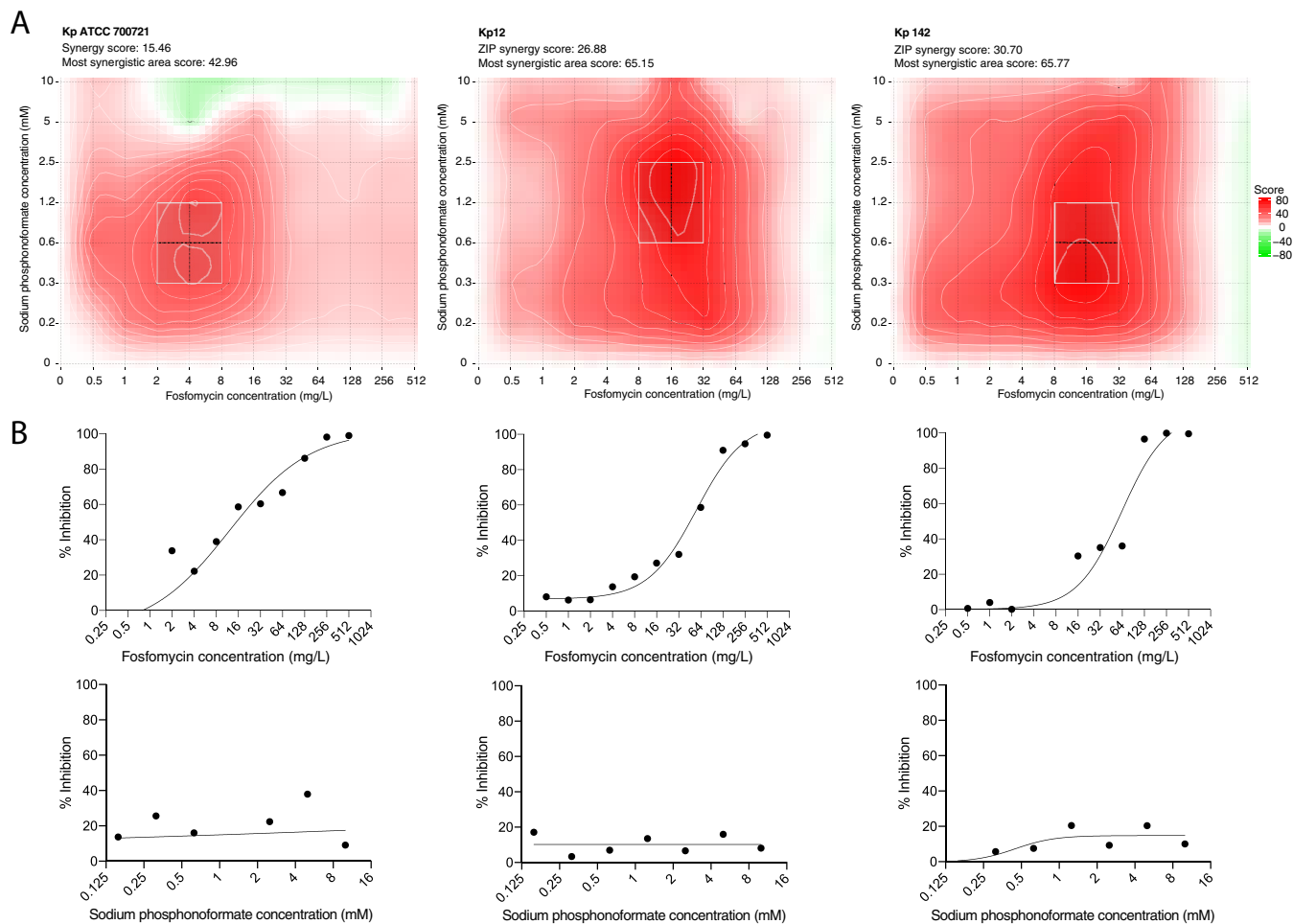
Nevertheless, the contribution of this fosfomycin resistance determinant alone and in combination with mutations affecting fosfomycin resistance-related genes remains unclear.

The present study aimed to determine the *in vitro* interplay between the main fosfomycin resistance determinants and fosfomycin resistance in *K. pneumoniae*.

(This study was presented in part at ECCMID 2019; Amsterdam, Netherlands [poster presentation P1903].)

## RESULTS

**Sequences of fosfomycin resistance-related genes.** The results for the fosfomycin resistance-related proteins (GlpT, UhpT, FosA, CyaA, Crp, PtsI, MurA, UhpA, UhpB, and UhpC) after *de novo* sequencing of the 12 *K. pneumoniae* isolates are shown in Table 1. No amino acid changes were found in CyaA, Crp, MurA, or UhpA in these clinical strains compared with *K. pneumoniae* ATCC 700721. Apart from polymorphisms with activity whose significance is unknown, insertions in GlpT were found in Kp58 (A261\_N262insA), Kp88 (A261\_N262insA), and Kp108 (Y258\_I259insA) and



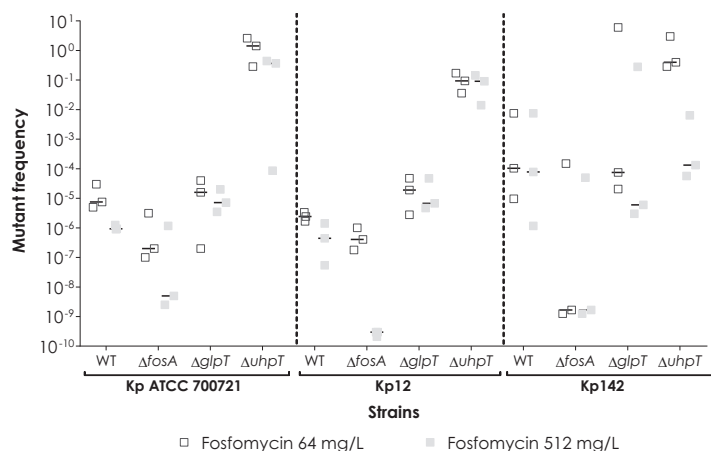
**FIG 1** (A) Synergistic activity of fosfomycin in combination with PPF against *K. pneumoniae* ATCC 700721, Kp12, and Kp142 strains. Red and green areas represent synergy (synergy score greater than +10) and antagonism (less than -10), respectively. White rectangles show the maximum synergy area. (B) Fosfomycin and PPF dose-response curves.

deletions were detected in Kp86 (*I260\_A261del*). The clinical Kp88 isolate also showed a truncated UhpT protein due to a premature stop codon.

**Fosfomycin susceptibility.** The fosfomycin MICs for the isogenic collection and clinical isolates are shown in Table 1. The modal MIC of the clinical isolates was 32 mg/liter, and the fosfomycin MICs ranged from 16 to  $\geq 1,024$  mg/liter. For the isogenic mutants, similar results were obtained for *K. pneumoniae* ATCC 700721, Kp12, and Kp142. The deletion of *glpT* showed no increase in MIC relative to that of the wild-type (WT) strain (32 mg/liter), while inactivation of *uhpT* (MIC of  $\geq 1,024$  mg/liter) led to a  $\geq 32$ -fold increase. Deletion of *fosA* caused a MIC change to 1 mg/liter, a 32-fold decrease with respect to that of the wild type.

The addition of 0.623 mM PPF reduced the MIC values of fosfomycin against all clinical isolates between 2- and 8-fold compared with the absence of PPF. The  $\Delta uhpT$  and  $\Delta fosA$  strains in the isogenic collection showed no decrease in fosfomycin MIC with the addition of PPF. Also, the fosfomycin MICs against Kp12 and Kp142  $\Delta fosA$  strains were 4- and 8-fold higher, respectively. Finally,  $\Delta glpT$  mutants of *K. pneumoniae* ATCC 700721 and Kp12 showed a 4-fold reduction in the fosfomycin MIC.

**Synergy assays.** The combination of fosfomycin and PPF showed synergistic activity against *K. pneumoniae* ATCC 700721, Kp12, and Kp142 strains (Fig. 1). According to the synergy score, the average (and maximum) proportions of bacterial response attributable to the drug interaction were 15.46 (42.96), 26.88 (65.15), and 30.7 (65.77) for *K. pneumoniae* ATCC 700721, Kp12, and Kp142, respectively. This maximum synergistic



**FIG 2** Fosfomycin-resistant mutant frequencies of *K. pneumoniae* ATCC 700721, Kp12, and Kp142 wild-type and isogenic mutant strains. Empty and full boxes show individual results, and black lines represent the median values of the three replicates.

area occurred in fosfomycin ranges of 2 to 8 mg/liter for *K. pneumoniae* ATCC 700721 and 8 to 32 mg/liter for Kp12 and Kp142 and in PPF ranges of 0.3 to 1.2 mM for *K. pneumoniae* ATCC 700721 and Kp142 and 0.6 to 2.5 mM for Kp12.

**Mutant frequencies.** The results of the mutant frequency estimates are shown in Fig. 2. The lowest fosfomycin resistance mutant frequencies were found among  $\Delta fosA$  mutants, with a decrease in frequency from  $1.69 \times 10^{-1}$  to  $1.60 \times 10^{-5}$  at 64 mg/liter and from  $5.38 \times 10^{-3}$  to  $2.13 \times 10^{-5}$  at 512 mg/liter relative to their wild-type strains. In terms of fosfomycin selection of mutants, small or no differences were observed between  $\Delta glpT$  and wild-type strains at 64 or 512 mg/liter. The  $\Delta uhpT$  mutation showed a frequency of close to 1, confirming a uniform population with a MIC above the selecting conditions, i.e., 64 or 512 mg/liter of fosfomycin. Addition of PPF showed no effect on mutant frequencies (see Fig. S1 in the supplemental material).

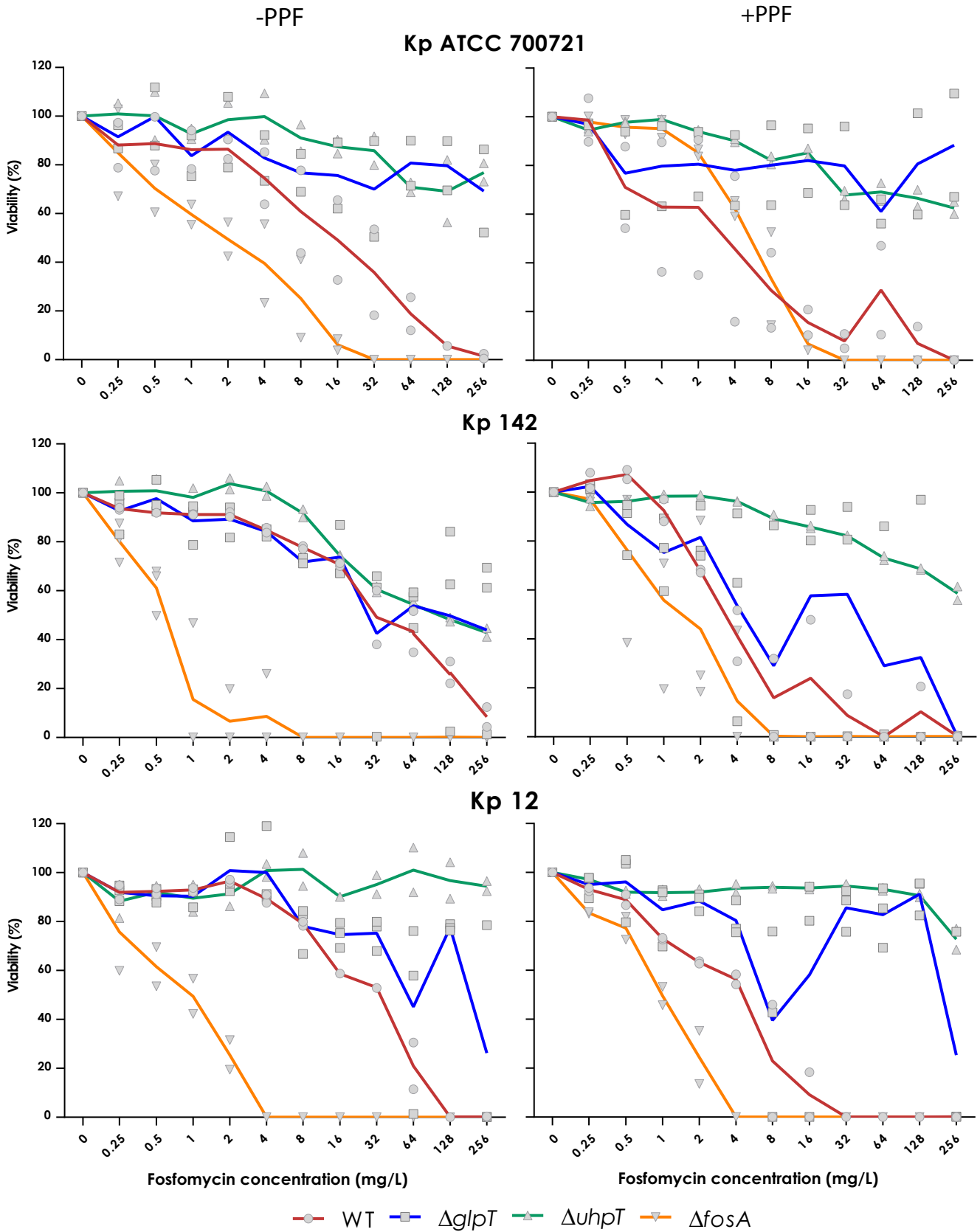
**Bacterial growth monitoring.** Figure 3 and Fig. S2 show the results for 24-h-growth monitoring assays, expressed as percentage of bacterial viability at each fosfomycin concentration used. The experiment was carried out with the isogenic collection and clinical isolates.

With respect to the isogenic collection of mutants (Fig. 3),  $\Delta fosA$  strains showed the highest susceptibility after fosfomycin exposure, with absence of growth at concentrations of 32, 8, and 4 against *K. pneumoniae* ATCC 700721, Kp12, and Kp142, respectively. High viability of  $\Delta glpT$  and  $\Delta uhpT$  mutants was observed across the range of fosfomycin concentrations tested. Finally, the addition of PPF did not reduce the viability of any mutant, except for the Kp12  $\Delta glpT$  mutant.

With respect to the wild-type clinical isolates, in the susceptible strains without known fosfomycin resistance-related mutations (*K. pneumoniae* ATCC 700721, Kp12, Kp28, and Kp142), no viability was observed at 256, >256, 256, and 128 mg/liter, respectively (Fig. S2). The addition of PPF showed an increase in fosfomycin activity, reducing by  $\geq 3 \log_2$  dilutions the fosfomycin concentration able to eliminate viable bacteria. Despite the fact that the isolates were susceptible (Kp58 and Kp88), but had mutations in *GlpT*, none of the fosfomycin concentrations tested were able to eradicate bacterial growth. Similar results were found with the highly resistant strains (Kp86 and Kp108). No differences in viability were observed with the addition of PPF against Kp58, Kp86, Kp88, and Kp108.

**Time-kill assays.** *K. pneumoniae* ATCC 700721, Kp12, Kp142, and their derivatives were evaluated at two concentrations of fosfomycin (64 and 307 mg/liter), with and without 0.623 mM PPF. The results of the time-kill assays are shown in Table 2 and Fig. S3, S4, and S5.

All the tested strains showed the emergence of bacterial subpopulations able to



**FIG 3** Viability of *K. pneumoniae* ATCC 700721, Kp12, and Kp142 wild-type and isogenic mutant strains against fosfomycin concentrations from 0 to 256 mg/liter, with and without 0.623 mM PPF after 24 h. Lines stand for mean values of measured viability. Symbols represent single results of the replicates.

**TABLE 2** Time-kill results for *K. pneumoniae* ATCC 700721, Kp12, and Kp142 wild-type and isogenic mutant strains using 64 and 307 mg/liter of fosfomycin, alone and in combination with 0.623 mM PPF<sup>a</sup>

	Fosfomycin concentration	Time (h)	KpATCC				Kp12				Kp142			
			WT	$\Delta fosA$	$\Delta glpT$	$\Delta uhpT$	WT	$\Delta fosA$	$\Delta glpT$	$\Delta uhpT$	WT	$\Delta fosA$	$\Delta glpT$	$\Delta uhpT$
No PPF	64 mg/L	2	-1.79	-1.16	-1.69	-0.34	-1.43	-2.39	-1.64	0.35	-1.74	-3.48	-3.27	-0.21
		4	-1.40	-1.42	-1.92	-0.41	-2.60	-3.94	-2.28	1.44	-2.75	-4.28	-1.94	1.33
		8	-1.17	-1.82	1.69	0.47	-1.03	-4.84	0.25	2.80	-1.99	-4.13	1.15	2.06
		24	3.37	-2.35	4.12	3.80	3.16	-1.88	3.55	3.26	2.94	-4.04	3.93	3.74
	307 mg/L	2	-1.41	-1.33	-1.66	-1.59	-3.37	-3.06	-3.91	-0.28	-2.59	-2.44	-2.28	-1.85
		4	-2.19	-1.64	-1.95	-1.29	-3.18	-4.08	-2.85	0.84	-3.22	-3.48	-2.05	-2.04
		8	-3.19	-1.94	2.01	0.92	-1.24	-4.08	-0.17	2.65	-3.50	-4.13	1.30	0.59
		24	-0.44	-2.10	4.06	3.95	2.57	-4.08	2.30	2.45	-5.02	-4.13	3.99	3.79
PPF 0.623mM	64 mg/L	2	-2.15	-2.46	-2.47	-0.56	-2.04	-2.79	-1.81	0.64	-1.97	-2.87	-2.25	0.63
		4	-2.60	-4.16	-2.69	0.47	-2.89	-4.33	-2.49	1.50	-2.14	-5.11	-2.47	1.20
		8	-0.80	-1.57	0.76	0.33	-1.64	-3.58	-0.31	2.74	-2.17	-3.14	0.83	2.67
		24	3.62	-0.80	3.81	3.35	3.11	-0.30	3.59	3.32	2.31	0.38	3.83	4.29
	307 mg/L	2	-2.64	-3.53	-1.79	-1.00	-2.50	-2.52	-1.93	-0.31	-2.84	-4.27	-2.16	-0.84
		4	-4.15	-4.96	-2.54	-1.03	-4.15	-5.04	-2.35	0.01	-2.78	-5.27	-2.23	0.28
		8	-3.21	-4.96	0.85	0.47	-3.85	-5.04	-0.03	2.06	-3.08	-5.27	0.71	0.11
		24	0.36	-0.32	3.55	3.92	2.92	-2.43	3.66	3.77	-1.04	-3.72	3.84	6.13

<sup>a</sup>The results are represented as differences (log<sub>10</sub> CFU per milliliter) relative to the initial time point (0 h). Green indicates a >3-log<sub>10</sub> CFU/ml decrease, yellow a 3- to 0-log<sub>10</sub> CFU/ml decrease, and red no bacterial reduction. WT, wild type.

grow at 64 mg/liter fosfomycin in the control tubes (assays without fosfomycin). In all these cases, subpopulations did not displace the main bacterial population. No differences were observed with the addition of PPF.

Fosfomycin (64 mg/liter) showed bactericidal activity (>3-log CFU/ml decrease) against Kp12  $\Delta fosA$  (at 4 and 8 h), Kp142  $\Delta fosA$  (from 0 to 24 h), and Kp142  $\Delta glpT$  (at 2 h). Fosfomycin reduced the bacterial burden of WT and  $\Delta glpT$  strains in the first 8 h and 4 h, respectively.  $\Delta uhpT$  mutants showed mild (*K. pneumoniae* ATCC 700721 and Kp142) or no (Kp12) killing at 64 mg/liter of fosfomycin at the beginning of the assay, in the first 4 h. All the strains in the isogenic collection, except for  $\Delta fosA$  *K. pneumoniae* ATCC 700721 and Kp142, regrew after 24 h at this concentration due to the emergence of resistant subpopulations.

Compared with the assay with 64 mg/liter of fosfomycin alone, the addition of PPF showed bactericidal activity against *K. pneumoniae* ATCC 700721 ( $\Delta fosA$ ) at 4 h and regrowth of Kp142 ( $\Delta fosA$ ) after 24 h.

After increasing the fosfomycin concentration to 307 mg/liter, only higher activity against WT strains and prevention of bacterial regrowth of  $\Delta fosA$  (Kp12 and Kp142 strains) were observed.

The addition of PPF increased fosfomycin activity at this concentration, with bactericidal activity against the *K. pneumoniae* ATCC 700721 (WT) strain at 4 h and the Kp12 ( $\Delta fosA$ ) strain at 2 to 8 h. Kp12 ( $\Delta fosA$ ) and Kp142 (WT) showed bacterial regrowth after 24 h relative to the assay without PPF. All the recovered strains showed fosfomycin MICs of >1,024 mg/liter.

**DISCUSSION**

The spread of multidrug-resistant bacteria is becoming a crucial public health problem (2). Fosfomycin has recently aroused great interest for the treatment of severe infections caused by *K. pneumoniae* (13, 14), although its activity is often limited by multiple mechanisms, including transporter defects, target modifications, and *fosA*-mediated inactivation. The impact of fosfomycin-inactivating enzymes on fosfomycin resistance among *Enterobacteriaceae* has been widely studied from different perspectives (13, 14). In this sense, various studies have looked for compounds able to reduce or inactivate their activity against fosfomycin (15, 16). Nevertheless, the combination of these determinants together with commonly observed mutations affecting fosfomycin intake has not been widely studied.



The present study evaluated the role of specific fosfomycin resistance determinants present in *K. pneumoniae* and their impact on the emergence of highly resistant strains during *in vitro* fosfomycin exposure. It also investigated a potential therapeutic approach using the FosA inhibitor sodium phosphonoformate, aimed at increasing fosfomycin susceptibility in *K. pneumoniae* clinical isolates.

In our isogenic *K. pneumoniae* collection of fosfomycin resistance-related genes, a baseline fosfomycin MIC of 32 mg/liter was observed for ATCC 700721, Kp12, and Kp142. Inactivation of *glpT* did not increase fosfomycin resistance relative to that of the wild-type strains. This phenotype has previously been observed in *E. coli* due to the use of glucose-6-phosphate in susceptibility assays (1, 17). Under these conditions, *uhpT* expression masks other fosfomycin resistance-related mutations, especially those related to the glycerol-3-phosphate transporter. On the other hand, inactivation of *uhpT* significantly increased the fosfomycin MIC ( $\geq 1,024$  mg/liter). The likely explanation for the reduced susceptibility is reduced uptake together with fosfomycin inactivation by the chromosomally mediated FosA.

Similar susceptibility results were found among *fosA* mutants. The inactivation of this chromosomal resistance determinant produced a 32-fold reduction in the fosfomycin MIC with respect to that of the wild-type strains. This change in susceptibility matches the modal MIC observed in the EUCAST fosfomycin MIC distribution found in *E. coli* (1 mg/liter and epidemiological cutoff [ECOFF] of 4 mg/liter), which lacks the chromosomal *fosA* gene (9, 18). The addition of PPF increased fosfomycin susceptibility in a variable way, although no activity was found in the *uhpT* mutant. This effect would not be explained by an increase in mutant frequency caused by PPF. Nevertheless, no differences in selection of rifampicin-resistant mutants were observed. Another plausible explanation is that PPF may compete with fosfomycin for transportation via the UhpT transporter, and this effect would be more evident in a strain lacking *fosA*, although this hypothesis was not studied.

With respect to the pharmacological approach for inhibiting FosA activity, a synergy study was performed combining fosfomycin and PPF.

The maximum synergistic area occurred within the fosfomycin susceptibility range (2 to 8 mg/liter for *K. pneumoniae* ATCC 700721 and 8 to 32 mg/liter of fosfomycin for Kp12 and Kp142), using EUCAST susceptibility breakpoints for *E. coli* (19). This synergistic activity was also promoted with the addition of PPF in a range from 0.3 to 2.5 mM, which corresponds to human blood concentrations after administration of 90 mg/kg of body weight every 12 h (q12h) (mean  $\pm$  standard deviation [SD] for steady-state maximum concentration of drug in serum [ $C_{max}$ ],  $0.623 \pm 0.132$  mM) (20). Similar results were obtained by Ito et al. using agar dilution assays (12), in which they found an apparent lack of activity of PPF at concentrations of up to 0.667 mM against some clinical strains or transformants with high fosfomycin MIC values.

The growth monitoring assays showed increased fosfomycin activity when *fosA* was absent relative to the wild-type strain. Despite showing better fosfomycin activity with the addition of PPF, these results did not improve those obtained with  $\Delta fosA$  strains. These discrepancies could be explained as the inefficient activity of PPF blocking FosA or the degradation or inactivation of PPF during the assay.

With respect to the  $\Delta glpT$  mutants, fosfomycin activity was lower than for the wild-type strains, despite having similar MICs. These results were similar to those previously obtained by our group in *E. coli*, whereby highly resistant mutants emerged from  $\Delta glpT$  strains following the selection of additional mutations in loci associated with fosfomycin resistance (1). These results also fit the higher fosfomycin mutant frequencies observed in  $\Delta glpT$  strains than in wild-type strains. No improved effects were observed against  $\Delta uhpT$  mutants when the assays were supplemented with PPF.

Comparable results were obtained with the other clinical isolates. The effect of PPF was observed in strains with low MICs and in the absence of fosfomycin resistance-related mutations, whereas a lack of PPF efficacy was observed when fosfomycin MIC was high or  $\Delta glpT$  was present.

Overall, the time-kill assays showed results similar to those found in the growth assays. Inactivation of *fosA* greatly improved fosfomycin efficacy with bacterial

reductions of between 1 and  $5\log_{10}$  CFU/ml. The addition of PPF to the time-kill assays improved fosfomycin activity only in the first hours, but the emergence of highly resistant mutants occurred in all assays. Our study differs slightly from the results obtained by Ito et al. (12). In that study, using a single *K. pneumoniae* strain with fosfomycin MIC of 256 mg/liter, the authors found a bactericidal effect at 8 and 24 h at concentrations of 256 and 512 mg/liter but bacterial regrowth at 24 h with 128 mg/liter. The addition of PPF to this assay showed a bactericidal effect at all concentrations of fosfomycin tested, including 128 mg/liter.

In conclusion, strategies aimed at inactivating *fosA* activity through gene editing (21) or using pharmacological approaches are promising for increasing fosfomycin activity against *K. pneumoniae* strains. In this respect, the pharmacological route is the most plausible one, but further PK/PD models should be carried out to better assess the activity of FosA-inactivating compounds.

## MATERIALS AND METHODS

**Bacterial strains.** Seven clinical multidrug-resistant *K. pneumoniae* strains from the Andalusian Reference Laboratory for Molecular Typing of Nosocomial Pathogens (PIRASOA program) categorized as susceptible or resistant to fosfomycin by MicroScan WalkAway (Beckman Coulter, Indianapolis, IN) were used. *K. pneumoniae* ATCC 700721 was used as the reference strain.

The two clinical isolates (Kp12 and Kp142) with the lowest fosfomycin MIC values and the reference strain *K. pneumoniae* ATCC 700721 were selected for isogenic mutant construction.

**Whole-genome sequencing.** The 7 clinical isolates were subjected to whole-genome sequencing on the MiSeq platform (Illumina, San Diego, CA), and sequencing was performed in-house. For this, the libraries were prepared with the Nextera XT DNA library preparation kit, and sequencing was done with a V3 600-cycle reagent cartridge. Sequencing was achieved with at least  $30\times$  average coverage. Illumina sequences were assembled *de novo* using the CLC genomics Workbench (Qiagen, Netherlands). The genomes were annotated with Rapid Annotation using Subsystem Technology (RAST) (22). The fosfomycin resistance-related proteins (MurA, GlpT, UhpT, FosA, CyaA, Crp, PtsI, UhpA, UhpB, and UhpC) were compared with *K. pneumoniae* ATCC 700721 using the NCBI BLAST online application.

**Isogenic mutant construction.**  $\Delta fosA$ ,  $\Delta glpT$ , and  $\Delta uhpT$  mutants were constructed using the  $\lambda$ -red gene replacement method, described by Huang et al. (23). All the required primers and plasmids are listed in Table S1. Briefly, the genes of interest (*fosA*, *glpT*, and *uhpT*) were removed by homologous recombination using an apramycin resistance cassette flanked by two 60-bp homologous sequences of the desired gene using the L-arabinose (Sigma-Aldrich, Madrid, Spain)-inducible recombinase of the pACBSR-Hyg plasmid. FLP recombination target (FRT) sites were also included in the construction to remove the apramycin resistance cassette (using pFLP-Hyg) from the chromosome once the mutants had been constructed. All the mutants were confirmed by PCR with sequence-specific primers for each region.

**Susceptibility testing.** Fosfomycin *in vitro* activity was determined by the gradient strip method (Liofilchem Diagnostici, Italy) using Mueller-Hinton agar (MHA). EUCAST fosfomycin susceptibility breakpoints for *Enterobacteriales* were used (19).

In addition, fosfomycin susceptibility testing was performed in Mueller-Hinton agar containing 0.623 mM PPF (Clinigen Healthcare, Staffordshire, UK). This concentration was selected on the basis of the maximum synergy results obtained in the synergy assay and corresponding to the  $C_{max}$  values for dosing of 90 mg/kg q12h (20). Assays were performed in duplicate.

**Synergy assay.** Synergies between fosfomycin and PPF were studied against Kp12, Kp142, and *K. pneumoniae* ATCC 700721 using the checkerboard assay. Briefly, the synergy assay was performed with an inoculum of  $5 \times 10^5$  CFU/ml in 96-well plates with a final volume of 100  $\mu$ l per well. Assays were conducted using Mueller-Hinton broth (MHB) supplemented with 25 mg/liter of glucose-6-phosphate. Fosfomycin concentrations ranged from 0.5 to 512 mg/liter and PPF concentrations from 0.16 to 10 mM. Wells without fosfomycin or PPF were used as single-drug assays or growth controls. Bacterial densities were quantified spectrophotometrically by measuring optical density (OD) at 595 nm using an Infinite200 Pro plate reader at 24 h. Bacterial viability was calculated as the ratio of final bacterial OD to the final bacterial OD of the control growth well (without drug). A four-parameter log logistic model was fitted to the data to generate dose-response curves for fosfomycin and PPF. Drug combination responses were also plotted as heat maps to assess the therapeutic significance of the combination by identifying the concentrations at which the drug combination had maximum effect on bacterial growth inhibition. The degree of drug synergy over the full dose-response matrix was analyzed using the response surface model, zero interaction potency (ZIP) with the SynergyFinder package for R (24). Synergy assays were performed in triplicate. The summary synergy represents the average excess response due to drug interactions. A synergy score of less than  $-10$  was considered antagonistic, a range from  $-10$  to  $+10$  as additive, and greater than  $+10$  as synergistic (25).

**Mutant frequencies.** Fosfomycin-resistant mutant frequencies were assessed for *K. pneumoniae* ATCC 700721, Kp12, Kp142, and their isogenic mutants. As PPF is a pyrophosphate analogue, its role in interfering with the replication process was assessed by analyzing the frequency of rifampicin-resistant



spontaneous mutants in wild-type *K. pneumoniae* and *E. coli* MG1655 strains (as a control due to the absence of chromosomal *fosA*).

Mutant frequencies were determined in triplicate as previously described (1). Fosfomycin-resistant mutants were recovered in MHA plates supplemented with 25 mg/liter of glucose-6-phosphate (Sigma-Aldrich) and two concentrations of fosfomycin (64 and 512 mg/liter; Sigma-Aldrich). Rifampicin-resistant mutants were recovered after overnight incubation of the bacterial culture with and without PPF (0.623 mM) and then plated on MHA with 100 mg/liter of rifampicin (Sigma-Aldrich). Mutant frequencies were the ratio of mutant to total CFU.

**Bacterial growth monitoring.** Bacterial growth curves were performed with  $5 \times 10^5$  CFU/ml as the starting inoculum, using 96-well plates (Nunc Delta Surface; Thermo Scientific, MA) with a 200- $\mu$ l volume per well. Assays were conducted using MHB supplemented with 25 mg/liter glucose-6-phosphate, with or without 0.623 mM PPF. Fosfomycin concentrations ranged from 0.25 to 256 mg/liter. Bacterial growth was quantified spectrophotometrically (595 nm) every hour, for 24 h, with an Infinite200 Pro plate reader (Tecan Group AG, Männedorf, Switzerland). Assays were performed in triplicate.

**Time-kill assays.** Time-kill assays were conducted in duplicate using fosfomycin concentrations of 0 (as a growth control), 64, and 307 mg/liter (maximal concentration of fosfomycin in plasma after intravenous administration of 8 g q8h) (26) with 25 mg/liter of glucose-6-phosphate, with or without 0.623 mM PPF. Briefly, single overnight colonies of each strain were used to prepare the preinoculum in Mueller-Hinton II broth and incubated overnight with shaking at 37°C. The starting inoculum was set at  $5 \times 10^5$  CFU/ml in a final volume of 20 ml, and bacterial cultures were incubated at 37°C with shaking. The number of viable CFU was determined at 0, 2, 4, 8, and 24 h by serial dilution, followed by plating on MHA plates with or without 64 mg/liter fosfomycin and 25 mg/liter of glucose-6-phosphate. The number of colonies was counted after 24 h of incubation.

When bacterial regrowth was observed after 24 h, up to 3 colonies were selected to assess fosfomycin MIC gradient strips. The survivors were serially passaged three times on fosfomycin-free plates to assess the stability of the phenotype and the fosfomycin MIC was determined, as previously described.

## SUPPLEMENTAL MATERIAL

Supplemental material is available online only.

**SUPPLEMENTAL FILE 1**, PDF file, 0.8 MB.

## ACKNOWLEDGMENTS

Miriam Ortiz-Padilla is supported by a PFIS fellowship from Instituto de Salud Carlos III. This study was supported by the Plan Nacional de I+D+i 2013-2016 and Instituto de Salud Carlos III, Subdirección General de Redes y Centros de Investigación Cooperativa, Ministerio de Economía, Industria y Competitividad, Spanish Network for Research in Infectious Diseases (PI16/01824, REIPI RD12/0015/0010, and REIPI RD16/0016/0001), cofinanced by European Development Regional Fund A Way To Achieve Europe, Operative Program Intelligent Growth 2014-2020, and the Consejería de Igualdad, Salud y Políticas Sociales, Junta de Andalucía (PI-0044 to 2013).

The funders had no role in the design, collection of data, analysis and writing of the manuscript, or the decision to publish.

J.R.-B. has been scientific coordinator of a research project unrelated to the project funded by AstraZeneca and a speaker at accredited educational activities funded by Merck through unrestricted grants. J.R.-B. and A.P. received funding in kind for research from COMBACTE-NET (grant agreement 115523), COMBACTE-CARE (grant agreement 115620), and COMBACTE-MAGNET (grant agreement 115737) projects under the Innovative Medicines Initiative (IMI), the European Union and EFPIA companies.

## REFERENCES

- Ballester-Téllez M, Docobo-Pérez F, Portillo-Calderón I, Rodríguez-Martínez JM, Racero L, Ramos-Guelfo MS, Blázquez J, Rodríguez-Baño J, Pascual A. 2017. Molecular insights into fosfomycin resistance in *Escherichia coli*. *J Antimicrob Chemother* 72:1303–1309. <https://doi.org/10.1093/jac/dkw573>.
- Prestinaci F, Pezzotti P, Pantosti A. 2015. Antimicrobial resistance: a global multifaceted phenomenon. *Pathog Glob Health* 109:309–318. <https://doi.org/10.1179/2047773215Y.0000000030>.
- Docobo-Pérez F, Drusano GL, Johnson A, Goodwin J, Whalley S, Ramos-Martín V, Ballester-Téllez M, Rodríguez-Martínez JM, Conejo MC, Van Guilder M, Rodríguez-Baño J, Pascual A, Hope WW. 2015. Pharmacodynamics of fosfomycin: insights into clinical use for antimicrobial resistance. *Antimicrob Agents Chemother* 59:5602–5610. <https://doi.org/10.1128/AAC.00752-15>.
- Falagas ME, Maraki S, Karageorgopoulos DE, Kastoris AC, Mavromanolakis E, Samonis G. 2010. Antimicrobial susceptibility of multidrug-resistant (MDR) and extensively drug-resistant (XDR) Enterobacteriaceae isolates to fosfomycin. *Int J Antimicrob Agents* 35:240–243. <https://doi.org/10.1016/j.ijantimicag.2009.10.019>.
- Pitout JD, Laupland KB. 2008. Extended-spectrum  $\beta$ -lactamase-producing Enterobacteriaceae: an emerging public-health concern. *Lancet Infect Dis* 8:159–166. [https://doi.org/10.1016/S1473-3099\(08\)70041-0](https://doi.org/10.1016/S1473-3099(08)70041-0).
- Veve MP, Wagner JL, Kenney RM, Grunwald JL, Davis SL. 2016. Comparison of fosfomycin to ertapenem for outpatient or step-down therapy of extended-spectrum  $\beta$ -lactamase urinary tract infections. *Int J Antimicrob Agents* 48:56–60. <https://doi.org/10.1016/j.ijantimicag.2016.04.014>.
- Castañeda-García A, Blázquez J, Rodríguez-Rojas A. 2013. Molecular

- mechanisms and clinical impact of acquired and intrinsic fosfomycin resistance. *Antibiotics (Basel)* 2:217–236. <https://doi.org/10.3390/antibiotics2020217>.
8. Marger MD, Saier MH. 1993. A major superfamily of transmembrane facilitators that catalyse uniport, symport and antiport. *Trends Biochem Sci* 18:13–20. [https://doi.org/10.1016/0968-0004\(93\)90081-W](https://doi.org/10.1016/0968-0004(93)90081-W).
  9. Ito R, Mustapha MM, Tomich AD, Callaghan JD, McElheny CL, Mettus RT, Shanks RMQ, Sluis-Cremer N, Doi Y. 2017. Widespread fosfomycin resistance in gram-negative bacteria attributable to the chromosomal *fosA* gene. *mBio* 8:e00749-17. <https://doi.org/10.1128/mBio.00749-17>.
  10. Li YY, Zheng B, Li YY, Zhu S, Xue F, Liu J. 2015. Antimicrobial susceptibility and molecular mechanisms of fosfomycin resistance in clinical *Escherichia coli* isolates in mainland China. *PLoS One* 10:e0135269. <https://doi.org/10.1371/journal.pone.0135269>.
  11. Nakamura G, Wachino JI, Sato N, Kimura K, Yamada K, Jin W, Shibayama K, Yagi T, Kawamura K, Arakawa Y. 2014. Practical agar-based disk potentiation test for detection of fosfomycin-nonsusceptible *Escherichia coli* clinical isolates producing glutathione S-transferases. *J Clin Microbiol* 52:3175–3179. <https://doi.org/10.1128/JCM.01094-14>.
  12. Ito R, Tomich AD, McElheny CL, Mettus RT, Sluis-Cremer N, Doi Y. 2017. Inhibition of fosfomycin resistance protein FosA by phosphonoformate (foscarnet) in multidrug-resistant gram-negative pathogens. *Antimicrob Agents Chemother* 61. <https://doi.org/10.1128/AAC.01424-17>.
  13. Abbott IJ, Meletiadiis J, Belghanch I, Wijma RA, Kanioura L, Roberts JA, Peleg AY, Mouton JW. 2018. Fosfomycin efficacy and emergence of resistance among Enterobacteriaceae in an in vitro dynamic bladder infection model. *J Antimicrob Chemother* 73:709–719. <https://doi.org/10.1093/jac/dkx441>.
  14. Elliott ZS, Barry KE, Cox HL, Stoesser N, Carroll J, Vegesana K, Kotay S, Sheppard AE, Wailan A, Crook DW, Parikh H, Mathers AJ. 2019. The role of *fosA* in challenges with fosfomycin susceptibility testing of multispecies *Klebsiella pneumoniae* carbapenemase-producing clinical isolates. *J Clin Microbiol* 57:e00634-19. <https://doi.org/10.1128/JCM.00634-19>.
  15. Thirumal Kumar D, Lavanya P, George Priya Doss C, Tayubi IA, Naveen Kumar DR, Francis Yesurajan I, Siva R, Balaji V. 2017. A molecular docking and dynamics approach to screen potent inhibitors against fosfomycin resistant enzyme in clinical *Klebsiella pneumoniae*. *J Cell Biochem* 118:4088–4094. <https://doi.org/10.1002/jcb.26064>.
  16. Tomich AD, Klontz EH, Deredge D, Barnard JP, McElheny CL, Eshbach ML, Weisz OA, Wintropde P, Doi Y, Sundberg EJ, Sluis-Cremer N. 2019. Small-molecule inhibitor of FosA expands fosfomycin activity to multidrug-resistant Gram-negative pathogens. *Antimicrob Agents Chemother* 63:e01524-18. <https://doi.org/10.1128/AAC.01524-18>.
  17. Portillo-Calderón I, Ortiz-Padilla M, Rodríguez-Martínez JM, de Gregoriolaria B, Blázquez J, Rodríguez-Baño J, Pascual A, Docobo-Pérez F. 2020. Contribution of hypermutation to fosfomycin heteroresistance in *Escherichia coli*. *J Antimicrob Chemother* 75:2066–2075. <https://doi.org/10.1093/jac/dkaa131>.
  18. European Committee on Antimicrobial Susceptibility Testing. 2020. Antimicrobial wild type distributions of microorganisms. <https://mic.euCAST.org/Eucast2/>.
  19. The European Committee on Antimicrobial Susceptibility Testing. 2020. Breakpoint tables for interpretation of MICs and zone diameters. Version 10.0. <http://www.euCAST.org>.
  20. Spanish Agency of Medicines and Medical Devices (Agencia española del medicamento y productos sanitarios, AEMPS). 2020. Ficha técnica: foscavir 24 mg/ml solución para perfusión. Agencia Española de Medicamentos y Productos Sanitarios (AEMPS), Madrid, Spain. [https://cima.aemps.es/cima/pdfs/es/ft/59712/FT\\_59712.pdf](https://cima.aemps.es/cima/pdfs/es/ft/59712/FT_59712.pdf).
  21. Kim J-S, Cho D-H, Park M, Chung W-J, Shin D, Ko KS, Kweon D-H. 2016. CRISPR/Cas9-mediated re-sensitization of antibiotic-resistant *Escherichia coli* harboring extended-spectrum  $\beta$ -lactamases. *J Microbiol Biotechnol* 26:394–401. <https://doi.org/10.4014/jmb.1508.08080>.
  22. Aziz RK, Bartels D, Best AA, DeJongh M, Disz T, Edwards RA, Formsma K, Gerdes S, Glass EM, Kubal M, Meyer F, Olsen GJ, Olson R, Osterman AL, Overbeek RA, McNeil LK, Paarmann D, Paczian T, Parrello B, Pusch GD, Reich C, Stevens R, Vassieva O, Vonstein V, Wilke A, Zagnitko O. 2008. The RAST Server: Rapid Annotations using Subsystems Technology. *BMC Genomics* 9:75. <https://doi.org/10.1186/1471-2164-9-75>.
  23. Huang TW, Lam I, Chang HY, Tsai SF, Palsson BO, Charusanti P. 2014. Capsule deletion via a  $\lambda$ -Red knockout system perturbs biofilm formation and fimbriae expression in *Klebsiella pneumoniae* MGH 78578. *BMC Res Notes* 7:13. <https://doi.org/10.1186/1756-0500-7-13>.
  24. Yadav B, Wennerberg K, Aittokallio T, Tang J. 2015. Searching for drug synergy in complex dose-response landscapes using an interaction potency model. *Comput Struct Biotechnol J* 13:504–513. <https://doi.org/10.1016/j.csbj.2015.09.001>.
  25. Ianevski A, Giri AK, Aittokallio T. 2020. SynergyFinder 2.0: visual analytics of multi-drug combination synergies. *Nucleic Acids Res* 48:W488–W493. <https://doi.org/10.1093/nar/gkaa216>.
  26. Pfausler B, Spiss H, Dittrich P, Zeitlinger M, Schmutzhard E, Joukhadar C. 2004. Concentrations of fosfomycin in the cerebrospinal fluid of neurointensive care patients with ventriculostomy-associated ventriculitis. *J Antimicrob Chemother* 53:848–852. <https://doi.org/10.1093/jac/dkh158>.